J Mol Model (2012) 18:3003–3012
DOI 10.1007/s00894-011-1296-9

ORIGINAL PAPER

High-pressure phase transition and thermoelastic properties of europium chalcogenides

Dinesh C. Gupta · Kailash C. Singh

Received: 10 May 2011 / Accepted: 25 October 2011 / Published online: 26 November 2011

Abstract The pressure-induced crystal properties of Eu chalcogenides were investigated using two different models: a modified charge-transfer potential model consisting of Coulomb screening due to the delocalization of the *f* electron of the rare earth atom, and modified by covalency and zero-point energy effects along with attractive and repulsive interactions; and a charge-transfer model that excluded the covalency and zero-point energy effects in the previous model. Both models were used to visualize the effect of covalency on the mechanism of interaction of the constituent atoms. Eu chalcogenides transform from the $Fm\bar{3}m$ to the $Pm\bar{3}m$ phase under the influence of sufficient pressure (P_T= 39.52, 21.01, 14.31, and 10.58 GPa), and their equations of state indicated decreases in volume during this phase transition of 6.38, 12.32, 12.76, and 11.15%, respectively, for EuO, EuS, EuSe, and EuTe. The results obtained from the models were in good agreement with corresponding experimental data. The elastic constants and Debye temperatures were also computed at normal and high pressures. Both of the models were found to be capable of successfully explaining these properties.

Keywords Eu chalcogenides · Structural properties · Equation of state · Phase transition · Elastic constants · Debye temperature

D. C. Gupta (✉) · K. C. Singh
Condensed Matter Theory Group, School of Studies in Physics,
Jiwaji University,
Gwalior 474 011 MP, India
e-mail: sosfizix@yahoo.co.in

Introduction

Recently, rare-earth compounds (RECs) have drawn much interest from materials scientists due to their intricate electronic, magnetic, optical, dielectric, and phonon properties, which result from the presence of highly correlated outer electrons (*f* electrons). These compounds have potential applications as spintronic and spin-filtering devices. The pressure–volume behavior of EuX (X=O, S, Se, or Te) is somewhat different from that of the other members of the REC family. Several high-pressure studies have been performed on these compounds, and it ws observed that they undergo a first-order transition from a sixfold-coordinated NaCl (B1) structure with space group $Fm\bar{3}m$ to an eightfold-coordinated CsCl (B2) structure with space group $Pm\bar{3}m$ [1–18]. Compounds where the Eu ion is in a divalent state (Eu^{2+}) are technologically important semiconducting materials, while compounds where the Eu ion belongs to the trivalent state (Eu^{3+}) due to the promotion of the *f* electron are metallic. Among these compounds, EuO is the only one that exhibits a valence transformation from 2+ to 3+ due to the promotion of a 4*f* electron into the 5*d* conduction band in Eu under pressure [3–6]. This electronic transition is isostructural (B1→B1′) near 30 GPa, but the lattice parameter contracts rapidly at a pressure of 40 GPa, and this is soon followed by the B1′→B2 structural transition [4–6]. However, other compounds of this family do not undergo this isostructural transition. They show only a B1 → B2 transition at 21.5, 14.5, and 11 GPa for EuS, EuSe, and EuTe, respectively [5, 6]. They exhibit normal behavior, more or less similar to that of ionic solids. Rooymans [7] has reported a valence transition in EuTe at ~3 GPa.

Eu chalcogenides show magnetic properties at low temperatures: EuO and EuS behave as ferromagnetic

semiconductors, while EuSe and EuTe are antiferromagnetic. A study of the structural and elastic properties of these compounds had been reported in the literature [8–18]. The Debye temperatures of Eu compounds have been reported by Shapira et al. [11], Benbattouche et al. [13], and Subhadra et al. [14].

The present article deals with the development of an improved potential model that incorporates proper crystal interactions: long-range (LR) Coulomb attraction and Coulomb screening due to *f* electrons of the rare-earth ion/atom, i.e., charge-transfer or many-body interactions (CTI or MBI) [19, 20] modified by covalency effects [21]; and short-range (SR) repulsion extending up to the second-nearest neighbors and represented by a Hafemeister and Flygare (HF) type potential [22]. Since these compounds are partially covalent in nature, covalency is included.

Recently, Gour et al. [17, 18], Varshney et al. [23], and Srivastava et al. [24] computed a few crystal properties of Eu and some other RECs, but many of these—especially the elastic properties, Cauchy's discrepancy, and the pressure variation—are not explained very well due to the exclusion of covalency and CTI from the expressions for the elastic moduli. These interactions are responsible for the Coulomb screening due to the delocalized *f* electrons in the rare-earth ion. The inclusion of the covalency effect improves the accuracy of the predicted values of the crystal properties under high pressure because this effect increases with pressure. The models used to explain the crystal properties in earlier works [17, 18, 23, 24] were rather basic, and excluding CTI, covalency, and zero-point (ZP) energy affected their potentials, which play an important role in defining the crystal properties of RECs, thus affecting the results obtained from such models. Their expressions for elastic moduli had $C_{12}=C_{44}$, which contradicted their results, as they showed Cauchy's discrepancy ($C_{12}\neq C_{44}$). Hence, the approach adopted for those models is not realistic qualitatively and quantitatively, and their results are unreliable.

To study the effect of these interactions on various crystal properties, we computed the cohesive, phase transition, elastic, and thermal properties of Eu compounds using two different models: a modified charge-transfer potential (MCTP) model; and a charge-transfer potential (CTP) model. Both of these models incorporate Coulomb attraction modified by Coulomb screening due to the delocalization of *f* electrons of the Eu ion, i.e., many-body or charge-transfer interactions along with covalency and ZP energy effects as well as SR repulsion extended up to the second-nearest neighbors. Since these compounds are partially covalent in nature, the Coulomb screening and covalency effects become quite important at high pressures. The calculations performed in the present models are valuable in cases where quantum mechanical modeling cannot be applied, e.g., in finite temperature simulations, etc. In such cases, the DFT-based quantum mechanical approach is extremely costly. Hence, the present calculations are quite important considering their ability to explain a variety of crystal properties using the same set of parameters. In the next section, we present a brief outline of the computational methodology used, along with the modified expressions. This is followed by a discussion of the results calculated using the two models.

Methodology

To understand the mechanism of interaction and to analyze the cohesive, phase-transition, elastic, and thermophysical properties at ambient and high pressures, we used MCTP and CTP models and compared the results from them. The CTP model is similar to the MCTP model except that covalency and ZP energy effects are excluded from it. Upon the application of pressure, the crystal volume decreases. The relative stabilities of the two competing phases (B1 and B2) were studied by minimizing the enthalpy $H(=E+PV)$ at zero pressure and high pressure. At the phase-transition pressure P_T, both phases coexist. In order to compute various crystal properties, the cohesive energy is expressed in the MCTP model as

$$E(r) = E_{\mathrm{Coul}} + E_{\mathrm{MCTI}} + E_{\mathrm{vdW}} + E_{\mathrm{HF}} + E_{\mathrm{ZP}}$$

or

$$E(r) = -\frac{\alpha_M Z^2 e^2}{r_{ij}} - 2n\frac{\alpha_M Z e^2}{r_{ij}} f_m(r_{ij}) - \frac{C}{r^6} - \frac{D}{r^8} + b\sum_{ij}\beta_{ij}\exp\left(\frac{\mathrm{r_i} + \mathrm{r_j} - \mathrm{r_{ij}}}{\rho}\right) + \frac{1}{2}h\upsilon. \quad (1)$$

The first term in the above equation is due to the LR Coulombic interaction. The second term represents the charge-transfer interaction (CTI) leading to the Coulomb screening effect due to the delocalization of the *f* electron of the cation, modified by the covalency effect. In order to understand the existence of CTI from the mechanism of charge transfer, we must consider three ions A, B, and C, represented by *lk*, *l′k′*, and *l″k″*, respectively, in an ionic crystal, as shown in Fig. 1. Their positions are such that C is the nearest neighbor (nn) of ion A and is separated by a distance *r*(*lk*, *l″k″*) from it, and B is another ion at a distance *r*(*lk*, *l′k′*) from A. During lattice vibrations, the electron shells of ions A and C overlap, and this overlap gives rise to the transfer of the following amount of charge: $q_k=\pm Zef_k(r(lk,l''k''))=\pm Zef_k(r)$. The amount of charge transferred is dependent on the degree of overlap, i.e., the interionic separation (*r*). Here, the function $f_k(r)$ is significant only between the nearest neighboring (nn) ions, and is expressed as $f_k(r) = \frac{Z_k}{Z} f(r)$,where $Z = |Z_k| = |Z_{k'}|$.

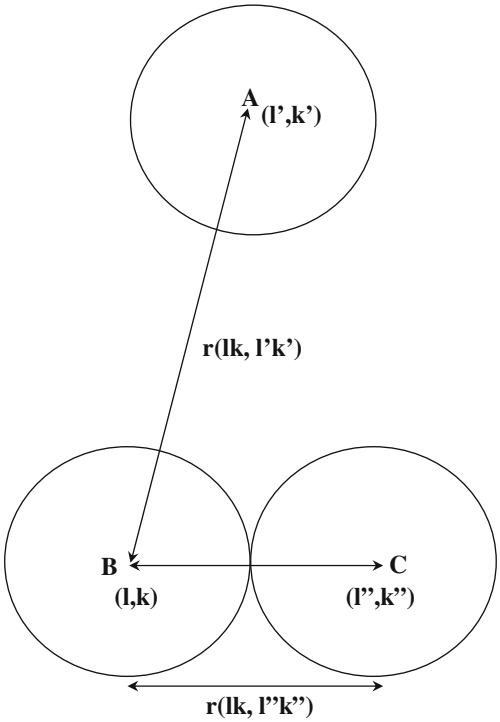

Fig. 1 Graphical representation of the many-body interaction or charge transfer mechanism

The occurrence of charge transfer modifies the ionic charge of A or C as

$$Z_{\mathrm{m}}e = Z_k e + nef_k(r(lk,l''k'')) = \pm Z_k e\left[1+\frac{2n}{Z}f(r(lk,l''k''))\right]^{1/2}.$$

Here, n is the number of nearest neighbors, and the term $[1+f(r_0)2n/Z]^2$has been approximated to $\left[1+\frac{2n}{Z}f(r_0)\right]^{1/2}$ due to the very small magnitude of $f(r)$. On this basis, we can express the total charge on ion B as $Z_{\mathrm{m}}e = \pm Z_{k'}e\left[1+\frac{2n}{Z}f(r(l'k',l'''k'''))\right]^{1/2}_{r=r_0}$,where ion $l'''k'''$, not shown in Fig. 1, is the nn of B. In view of the above descriptions, the Coulomb interaction energy between the ion pair A and B is modified to

$$\begin{aligned}E_{\mathrm{Coul}}(r(lk,l''k'')) &= \frac{e^2 Z_{\mathrm{m}k}Z_{\mathrm{m}k'}}{|r(lk,l'k')|}\\ &= \frac{e^2[Z_k+nf_k(r(lk,l''k''))][Z_{k'}+nf_{k'}(r(l'k',l'''k'''))]}{r|(lk,l'k')|}\\ &= \frac{Z_k Z_{k'}e^{\ 2}}{|r(lk,l'k')|}+\frac{ne^2}{|r(lk,l'k')|}\\ &\quad\times[Z_k f_{k'}(r(l'K',l'''k''')) + Z_{k'}f_k(r(lk,l''k''))]\\ &\quad + n^2e^2(|r(lk,l'k')|)^{-1}[f_k(r(lk,l''k''))f_{k'}(r(l'k',l'''k'''))]\end{aligned}$$

$$\begin{aligned}&= Z_k Z_{k'}e^2(|r(lk,l'k')|)^{-1} + ne^2(|r(lk,l'k')|)^{-1}[Z_k f_{k'}(r(l'K',l'''k''')) \\ &\quad + Z_{k'}f_k(r(lk,l''k''))] + n^2e^2(|r(lk,l'k')|)^{-1}[f_k(r(lk,l''k''))f_{k'}(r(l'k',l'''k'''))]\end{aligned} \tag{2}$$

Here, the first term is the well-known central two-body Coulomb potential. The second term has two parts specifying the contributions of the LR central type potential; the magnitude of this depends on the coordinates of the three atoms, so they can be referred to as three-body interactions. The last term arise from four-body interactions, and can be neglected in this formulation as it involves the product of two very small functions $f_k(r)$ and $f_{k'}(r)$. Due to the identical distributions of the ion pairs throughout the lattice, the same function $f(r(lk,l''k''))$ can be used to represent the charge transfer between each ion pair. Hence, the modified Coulomb energy expression can be written as

$$E_{\mathrm{Coul}}^{\mathrm{mod}} = E_{\mathrm{Coul}} + E_{\mathrm{CTI}}, \tag{3}$$

where

$$E_{\mathrm{Coul}} = \frac{e^2}{2}\sum_{lk}\sum_{l'k'}\frac{Z_k Z_{k'}}{|r(lk,l'k')|} \tag{4}$$

and

$$E_{\mathrm{CTI}} = e^2\sum_{lk}\sum_{l'k'}\sum_{l''k''}f(r(lk,l''k''))\frac{Z_k Z_{k'}}{|(r(lk,l'k'))|}, \tag{5}$$

which when solved gives

$$E_{\mathrm{CTI}}(r) = -\frac{2\alpha_{\mathrm{M}}e^2 Znf(r)}{r}. \tag{6}$$

Here, n is the number of nn, and $f(r)$ is the CTI parameter, which depends upon the overlap integrals. Motida [21] has proposed a method of modifying the CTI to include covalency effects. The second term in Eq. 1, E_{MCTI}, is due to the CTI modified for the covalency effect, and is calculated via

$$f_{\mathrm{m}}(r)(=f_{\mathrm{CTI}}(r)+f_{\mathrm{Cov}}(r)). \tag{7}$$

The value of the CTI parameter, which is dependent on the lattice constant, can be estimated by

$$f_{\mathrm{CTI}}(r) = f_0\exp(-r/\rho). \tag{8}$$

Here, f_0 is the CTI constant. The covalency term can be expressed as

$$f_{\mathrm{Cov}}(r) = \frac{4V_{sp\sigma}^2e^2}{r_0E_{\mathrm{g}}^3} \text{ and } 1-\left(\frac{e_{\mathrm{s}}^*}{e}\right) = n_{\mathrm{c}}. \tag{9}$$

Here, $V_{sp\sigma}$ denotes the transfer matrix between the anion (outermost f orbital) and the cation (lowest excited s state), E_{g} is the energy associated with the transfer of an electron from the f orbital of the anion to the s orbital of the cation, and e_{s}^* indicates the Szigeti effective charge [25] of the host crystal. n_{c} is the number of electrons transferred to the unoccupied orbital of the cation from the nearest anion. We can determine $V_{sp\sigma}^2/E_g^2$ using a hypothesis derived from

correlations between the hyperfine coupling constants of the transition metal impurity ions and the Szigeti effective charge e_s^* of the host crystal:

$$\frac{V_{sp\sigma}^2}{E_g^2} = \frac{n_c}{12}, \tag{10}$$

as used in the linear combination of atomic orbital (LCAO) approximation. The value of E_g (the energy associated with the transfer of an electron from anion to cation) was determined using

$$E_g = E - I + \frac{(2\alpha_M - 1)e^2}{r_0}. \tag{11}$$

Here, E denotes the electron affinity of the atom and I denotes the ionization potential of the rare-earth atom. We have defined the effective charge (ek^* and ek'^*) as appear in the LR Coulomb interaction between the nth cell of the ion (lk) and the ion ($l'k'$) as $E_{Coul} = e_k^* e_{k'}^* / r(lk, l'k')$ Here, $r(lk, l'k')$ denotes the separation between the anion and cation. We have also included attractive forces due to covalency, which arise upon neglecting the charge flow between ions due to the SR forces during lattice displacement. We then find that the effective charge (e^*) equals the Szigeti effective charge e_s^*, as

$$\left(\frac{e_s^*}{e}\right)^2 = \frac{9V\mu\omega_0^2(\varepsilon_0 - \varepsilon_\infty)}{4\pi e^2(\varepsilon_\infty + 2)^2}. \tag{12}$$

In the above expression, V denotes the unit cell volume, μ is the reduced mass of the ions, ω_0 is the infrared dispersion frequency, and ε_0 (ε_∞) are the static (optical) dielectric constants, which were obtained using the Lyddane–Sachs–Teller (LST) relation [26] $\frac{\omega_L^2}{\omega_T^2} = \frac{\varepsilon_0}{\varepsilon_\infty}$, where ω_L and ω_T are the longitudinal and transverse frequencies at the zone center. The LST relation is valid in the present MCTP model, and it is independent of the microscopic origins of the electrical polarization [27].

Hence, $E_{MCTI}(r)$ may be written as

$$E_{MCTI}(r) = -\frac{2\alpha_M e^2 Z n f_m(r)}{r}. \tag{13}$$

The third and fourth terms correspond to the van der Waals (vdW) energies due to dipole–dipole and dipole–quadruple interactions. The fifth term is the SR repulsive interaction potential extending up to the second-nearest neighbors, which is represented by a Hafemeister–Flygare (HF) type potential. The last term is the contribution due to the zero-point energy. Equation 1 can be further generalized to

$$E(r) = -\frac{\alpha_M Z_m^2 e^2}{r_{ij}} - \left[\frac{C}{r^6} + \frac{D}{r^8}\right] + b\sum_{ij}\beta_{ij}\, exp\left(\frac{r_i + r_j - r_{ij}}{\rho}\right) + \frac{1}{2}h\upsilon, \tag{14}$$

where $Z_m e = \pm e\left(Z^2 + 2nZf_m(r_{ij})\right)^{\frac{1}{2}}$ is the modified ionic charge. Here, α_M is the Madelung constant, Ze is the ionic charge, r_{ij} is the equilibrium interionic distance, and β_{ij}=1+(Z_i/n_i)+(Z_j/n_j) are the Pauling coefficients, where Z_i (Z_j) and n_i (n_j) are the valence and the number of outermost electrons in the respective ions, and r_i and r_j are the ionic radii of the cation and anion, respectively. C and D are the overall vdW coefficients estimated using the Slater–Kirkwood variational approach [28], b is the hardness parameter, ρ is the range parameter, h is Plank's constant, υ is the lattice frequency, and e is the elementary charge of the electron. The physical origin of the SR repulsion is the overlap of the closed electron shells. According to Pauli's exclusion principal, two electrons that both have all the same quantum numbers cannot exist in same state, so they repel each other during shell overlap. These repulsive forces increase strongly in the shell overlap region as the interionic separation (r) decreases.

The values of the SR parameters b_m (b) and ρ_m (ρ) were determined from the equilibrium condition $dE(r)/dr|_{r=r0}$=0) and the bulk modulus $d^2E(r)/dr^2$=$9KrB_T$, where K (=V/r^3) is a structure-dependent constant and B_T is the bulk modulus. The MCTP model was used to derive the corrected relations for elastic moduli, as described in the next section.

Second-order elastic constants (SOECs)

We derived expressions for the SOECs for the NaCl structure based on a method expressed elsewhere [20, 29] as follows:

$$C_{11} = \left(\frac{e^2}{4a^4}\right)\left\{-5.112Z_m^2 + A_1 + \frac{(A_2 + B_2)}{2} + \underline{9.3204Zaf_m'(r)}\right\} \tag{15}$$

$$C_{12} = \left(\frac{e^2}{4a^4}\right)\left\{1.391Z_m^2 + \frac{(A_2 - B_2)}{4} + \underline{9.3204Zaf_m'(r)}\right\} \tag{16}$$

$$C_{44} = \left(\frac{e^2}{4a^4}\right)\left\{1.391Z_m^2 + \frac{(A_2 - B_2)}{4}\right\} \tag{17}$$

$$C_{12} - C_{44} = \underline{9.3204\left(e^2/4a^4\right)Zaf_m'(r)},$$

where $B_1 + B_2 = -1.165Z_m^2$ as the equilibrium condition. Adopting a similar process, the expressions for the CsCl structure were also obtained:

$$C_{11} = \left(\frac{e^2}{4a^4}\right)\left\{0.7009Z_m^2 + \frac{(A_1 + 2B_1)}{6} + \frac{A_2}{2} + \underline{3.1337Zaf_m'(r)}\right\} \tag{18}$$

$$C_{12} = \left(\frac{e^2}{4a^4}\right)\left\{-0.5201Z_m^2 + \frac{(A_1 - B_1)}{6} + \underline{3.1337Zaf_m^{'}(r)}\right\} \quad (19)$$

$$C_{44} = \left(\frac{e^2}{4a^4}\right)\left\{-0.5201Z_m^2 + \frac{(A_1 - B_1)}{6}\right\} \quad (20)$$

$$C_{12} - C_{44} = \underline{3.1337\left(e^2/4a^4\right)Zaf_m^{'}(r)},$$

where $B_1 + B_2 = -0.3392Z_m^2$as the equilibrium condition, and $Z_m^2 = Z(Z + 2nf_m(r))$.

Here, A_i and B_i (i=1, 2) are the SR force constants for nn and nnn ions. These SR force constants can be derived from the SR potential. The underlined term in the above expressions is essential for explaining Cauchy's discrepancy in solids. We should note that the expression reported in earlier works [17, 18, 23, 24] actually leads to C_{12}=C_{44}, while the results given in those works show that $C_{12}\neq C_{44}$. On the other hand, the expressions derived by us are capable of correctly explaining Cauchy's discrepancy ($C_{12} - C_{44}\neq 0$) in terms of the modified CTI parameter. Our expressions for the SOECs give $C_{12} - C_{44}$=9.3204 $(e^2/4a^4)Zaf'_m(r)$ for the NaCl structure and $C_{12} - C_{44}$=3.1337$(e^2/4a^4)Zaf'_m(r)$ for the CsCl structure.

To compute the thermophysical properties, we computed the Debye temperature (θ_D) using the method reported by Guo et al. [30]. The higher derivatives of the CTI parameter $f(r)$, i.e., $af'(r)$, $a^2f'''(r)$, and $a^3f''''(r)$, were obtained from the analytical expression $f(r)$=$f_0e^{-r/\rho}$, as suggested by Cochran [31]. The method used to compute the model parameters is given in the following section.

Computation of model parameters

The present MCTP and CTP models incorporate only three model parameters: $b_m(b)$, $\rho_m(\rho)$, and $f_m(r)$ or $f(r)$. The expressions for the equilibrium condition ($dE(r)/dr|_{r=r0}$=0) and the bulk modulus ($d^2E(r)/dr^2$=$9KrB_T$) were used to evaluate these model parameters by a self-consistent method. The required input data at room temperature and the values of the model parameters thus computed are listed in Table 1. Both models were employed to predict lattice, harmonic, anharmonic, thermophysical, high-pressure phase-transition, equation of state (EOS), and other allied properties of the partially covalent RECs. It is clear from Table 1 that the model parameters obtained from the MCTP model are slightly higher than those obtained by the CTP model. This difference in values is due to the fact that the effects due to covalency and ZP energy are ignored in the latter model. Such variations in the values of the model parameters will naturally affect the crystal properties.

Results and discussion

Cohesive and phase-transition properties

In order to check the relative stabilities of the two competing phases, we minimized the enthalpy H(=$E(r)$+PV) in both (B1 and B2) phases using an iterative self-consistent technique in order to obtain optimized values for the lattice volume and enthalpies under ambient as well as high-pressure conditions. These values were obtained by performing variable-cell calculations at different external pressures and relaxing the unit cell simultaneously in every direction of the cube until the stress tensor was diagonal.

The enthalpy values computed in the MCTP (CTP) model approach equality at 39.52 (38.87), 21.01 (20.18), 14.31 (13.82), and 10.58 (10.23) GPa for EuO, EuS, EuSe, and EuTe, respectively. These values for the phase-transition pressure P_T(40, 21.5, 14.5, and 11 GPa) are reported in Table 2, and they are reasonably close to the experimental [4–6] values and more accurate than those obtained in earlier works [8, 9, 17, 18] and from our CTP model. The variation of P_T with the cation to anion ratio (r_c/r_a) in each model for Eu chalcogenides is plotted in Fig. 2. This figure shows that P_T decreases with decreasing r_c/r_a

Table 1 Input data r (10^{-10} m) and B_T (GPa), and model parameters b_m and b (in 10^{-19} J), ρ_m and ρ (in 10^{-10} m), and the CTI parameter $f_m(r)$ or $f(r)$ (no units) for Eu chalcogenides

Crystal	Input data		Model parameters					
			MCTP in present work			CTP in present work		
	r	B_T	b_m	ρ_m	$f_m(r)$	b	ρ	$f(r)$
EuO	2.57	110.00	0.1589	0.4745	−0.0252	0.1543	0.4643	−0.0108
EuS	2.98	61.00	0.1767	0.5147	−0.0296	0.1739	0.5023	−0.0187
EuSe	3.09	52.00	0.2246	0.5546	−0.0339	0.2231	0.5438	−0.0292
EuTe	3.30	40.00	0.2624	0.5868	−0.0383	0.2613	0.5842	−0.0343

Table 2 Equilibrium volumes V_{B1}, V_{B2} in 10^{-30} m^3, phase transition pressure P_T in GPa, % volume collapse $\Delta V(P_T)/V(0)$ at P_T, and compression ratio $V(P_T)/V(0)$ in the B1 phase for Eu chalcogenides

Crystal	V_{B1}	V_{B2}	P_T	$\Delta V(P_T)/V(0)$	$V(P_T)/V(0)$	Reference
EuO	33.95	31.33	39.52	6.38	0.75	Present work: MCTP
	33.16	24.64	38.87	6. 32	0.73	Present work: CTP
	33.95	–	40.00	6.50	0.77	Expt. [4, 5]
	–	–	19.3, 36 [17]	6.3, 7.7[17]	–	Others [8]
EuS	52.93	48.12	21.01	12.32	0.65	Present work: MCTP
	52.39	39.12	20.18	11.99	0.64	Present work: CTP
	52.93	–	21.50	12.50	0.66	Expt.[5]
	–	–	11.60	5.70	–	Others [8]
	43.44	–	27.03, 20 [17]	11.22, 12 [17]	0.80	Others [9]
EuSe	59.01	53.34	14.31	12.76	0.58	Present work: MCTP
	57.87	46.31	13.82	11.92	0.57	Present work: CTP
	59.01	–	14.50	12.80	0.59	Expt.[5]
	49.28	–	23.88, 15 [18]	10.57, 9.5 [18]	0.88	Others [9]
EuTe	71.65	64.33	10.58	11.15	0.57	Present work: MCTP
	70.57	57.88	10.23	10.87	0.55	Present work: CTP
	71.87	–	11.00	11.60	0.58	Expt.[5, 6]
	–	–	10.50	8.80	–	Others [18]

ratio from O to Te, indicating that the crystal becomes unstable at lower pressures due to the increased dominance of repulsive forces. The minor deviations in the values of the phase-transition properties may be due to differences in the internal energy or enthalpy computed from the CTP model as compared to the MCTP model. These differences are due to the exclusion of covalency and ZP energy effects from the CTP model.

The computed values for the relative volume $V(P)/V(0)$ in both phases are plotted in Figs. 3, 4, 5, and 6 to obtain the phase diagrams / EOS for the Eu compounds. It is clear from Fig. 3 that the volume of EuO decreases smoothly up to 39.52 GPa. At this pressure, an abrupt decrease in volume is observed, which is attributed to the first-order transformation due to the structural changes associated with the B1→B2 transition. Similar trends are observed in EuS,

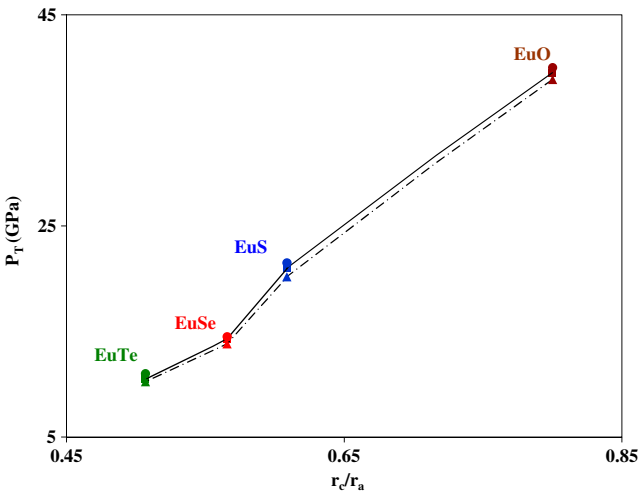

Fig. 2 The variation in the phase-transition pressure P_T with the cation–anion radius ratio r_c/r_a for Eu chalcogenides. The *squares* and *triangles* correspond to the MCTP and CTP models, respectively, while the *dots* refer to experimental data [4–6]

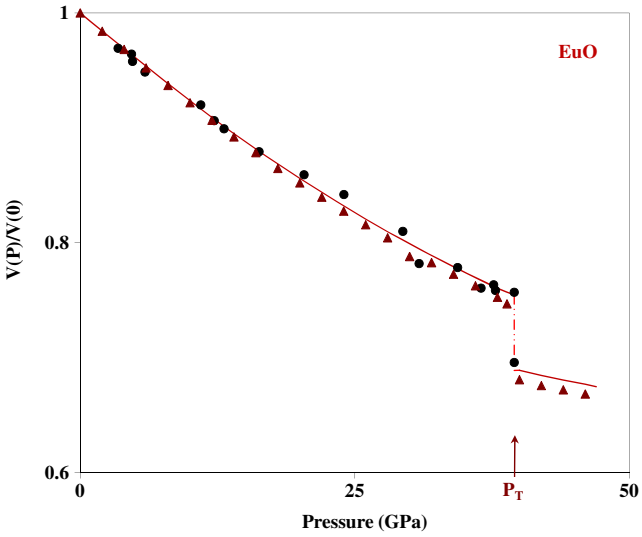

Fig. 3 The variation of the relative volume $V(P)/V(0)$ with pressure P for EuO. The *lines* and *triangles* correspond to the MCTP and CTP models, respectively, while the *dots* refer to experimental data [4]

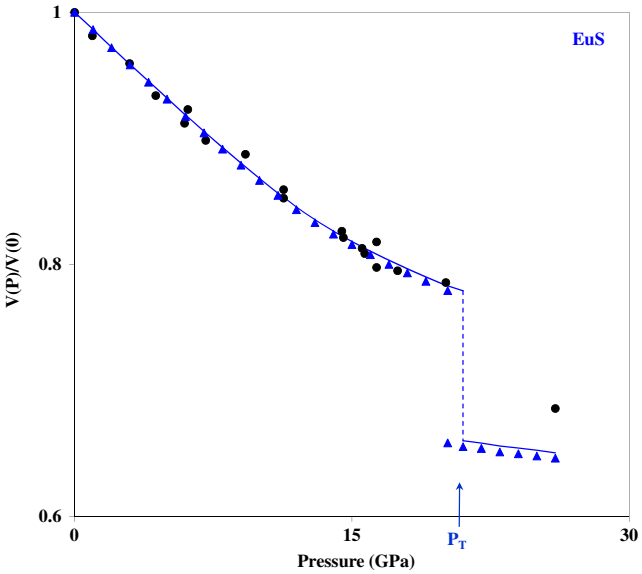

Fig. 4 The variation of the relative volume $V(P)/V(0)$ with pressure P for EuS. The *lines* and *triangles* correspond to the MCTP and CTP models, respectively, while the *dots* refer to experimental data [5]

EuSe, and EuTe but with different magnitudes of P_T. The EOS computed from the MCTP model shows good agreement with measured data [4–6] for all of the compounds, whereas the results of the CTP model show small deviations from the experimental values. The % volume collapse $\Delta V(P_T)/V(0)$ and the compression ratio $V(P_T)/V(0)$ at P_T in the B1 phase have also been included in Table 2. The computed values of % volume collapse and compression ratio in the B1 phase at P_T obtained from the present models are good agreement with the measured data,

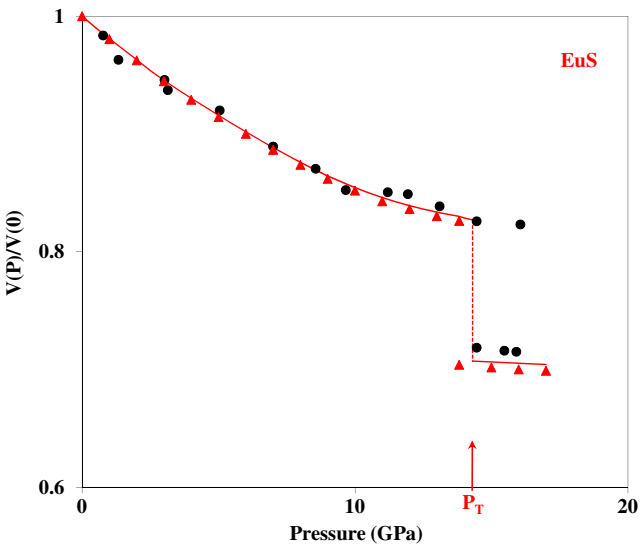

Fig. 5 The variation of the relative volume $V(P)/V(0)$ with pressure P for EuSe. The *lines* and *triangles* correspond to the MCTP and CTP models, respectively, while the *dots* refer to experimental data [5]

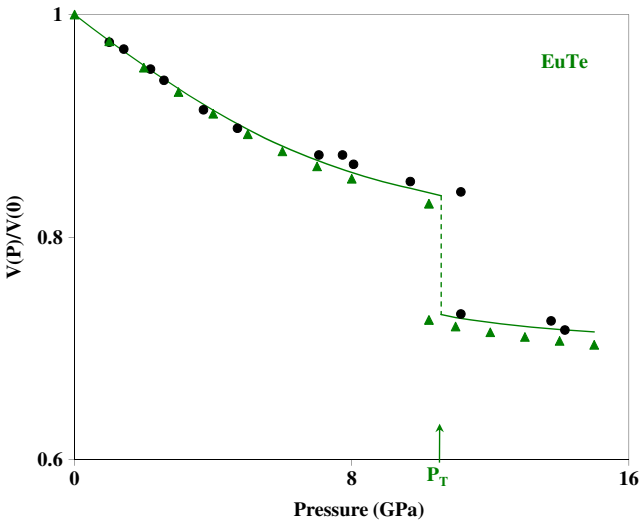

Fig. 6 The variation of the relative volume $V(P)/V(0)$ with pressure P for EuTe. The *lines* and *triangles* correspond to the MCTP and CTP models, respectively, while the *dots* refer to experimental data [6]

and are more accurate than those obtained by others [8, 9, 17, 18]. As the pressure increases the deviation increases, which shows that the covalency, CTI, and ZP energy effects become stronger with pressure.

To visualize the effect of pressure on the Eu–Eu interaction, we plotted the variation of the Eu–Eu distance in Fig. 7 for EuX compounds. The Eu–Eu distance varies linearly up to P_T in the B1 phase, and shows an abrupt drop at P_T, before again varying smoothly in the B2 phase in all of the compounds. It is also clear that the Eu–X distances in the B1 phase are slightly larger than the sum of the covalent radii of Eu (1.34 Å) and O (0.73 Å), S (1.02 Å), Se (1.16 Å), or Te (1.36 Å), while they are smaller than the sum of the atomic radius of Eu (2.04

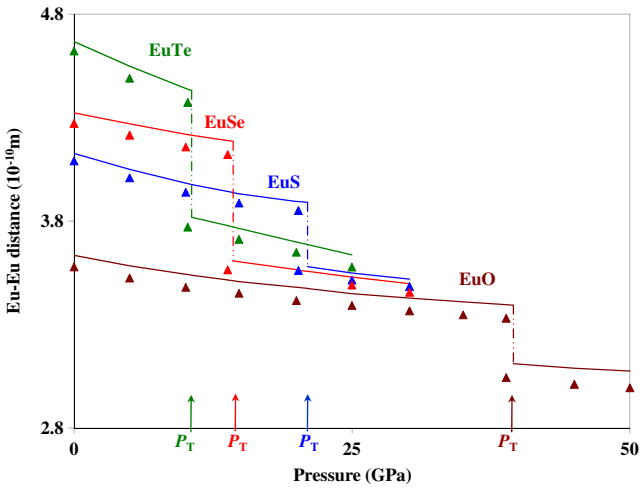

Fig. 7 Eu–Eu distances with pressure (P) for EuX (X=O, S, Se, Te). The *lines* and *triangles* correspond to the MCTP and CTP models, respectively

Table 3 Second-order elastic constants C_{11}, C_{12}, C_{44} and bulk modulus B_T (in GPa) for Eu chalcogenides

Parameters	EuO	EuS	EuSe	EuTe	Reference
C_{11}	198	133	118	97	Present work: MCTP
	196	131	116	94	Present work: CTP
	192, 192±6 [11]	131, 115±1 [13]	116	93.60	Exp. [10]
	251 [17]	211.06, 113.5 [17]	185.19, 118.8 [18]	63.8 [18]	Others [9]
C_{12}	44	17	15	9	Present work: MCTP
	43	16	14	8	Present work: CTP
	42.5, 42.5±8.5 [11]	11, 36±2 [13]	12.00	6.70	Exp. [10]
	55 [17]	10.47, 26 [17]	6.9, 27.7 [18]	23.1 [18]	Others [9]
C_{44}	57	26	23	17	Present work: MCTP
	56	26	23	16	Present work: CTP
	54.2, 54.2±1.3 [11]	27.3, 26±1 [13]	22.80	16.30	Exp. [10]
	52 [17]	174.25, 11.1,24 [17]	183.72, 18 [18]	6.8 [18]	Others [9]
B_T	95	55	49	38	Present work: MCTP
	94	55	48	37	Present work: MCTP
	110±5, 92±6 [11]	61±5, 63±1 [13]	52±5	40±5	Exp. [5, 6]
	92.33	51	46.66	35.66	Exp. [10]*
	–	77.36,53.6 [8], 68.48 [16]	66.33, 52.95 [15]	–	Others [9]

* Values were computed from the experimental data [10]

Å) and the covalent radius of X. Hence, the chemical bond between Eu and X is partially covalent in nature.

Elastic properties

Studying the elastic moduli provides essential information on the interaction mechanism of the constituents of the crystals. To obtain the values of the elastic moduli, the elastic strength, and their variations with pressure, we computed the SOECs for these compounds under ambient conditions; they are reported in Table 3, while their variations with pressure are plotted in Figs. 8, 9, and 10. It can be seen from Table 3 that our computed values satisfy all of the stability conditions (i.e., $C_{11} - C_{12}>0$; $C_{11}+2C_{12}>0$; $C_{11}>0$; and $C_{44}>0$) [32], and we can therefore say that the materials are mechanically stable in the B1 phase. The variation of B_T with pressure for EuX is depicted in Fig. 8. This figure shows that, under ambient conditions, the value of B_T decreases from O→Te due to the increasing interionic distance, which gives rise to a decrease in Coulomb energy and hence total energy. The variation of B_T indicates that EuTe is more compressible than the other members of this family. The

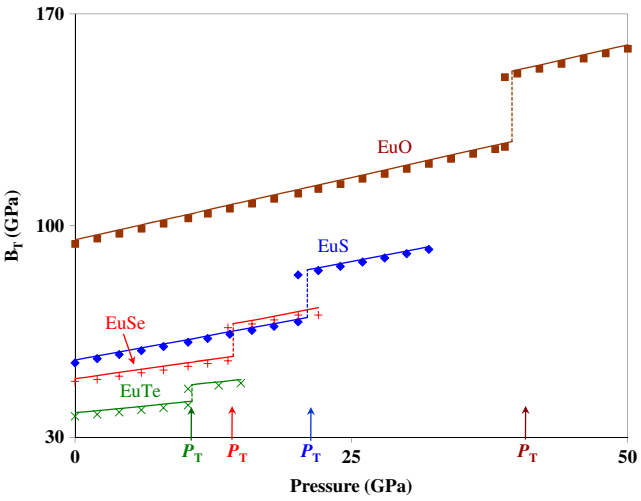

Fig. 8 The variation of B_T with pressure (P) for Eu chalcogenides. The *lines* correspond to the MCTP model and the *symbols* to the CTP model

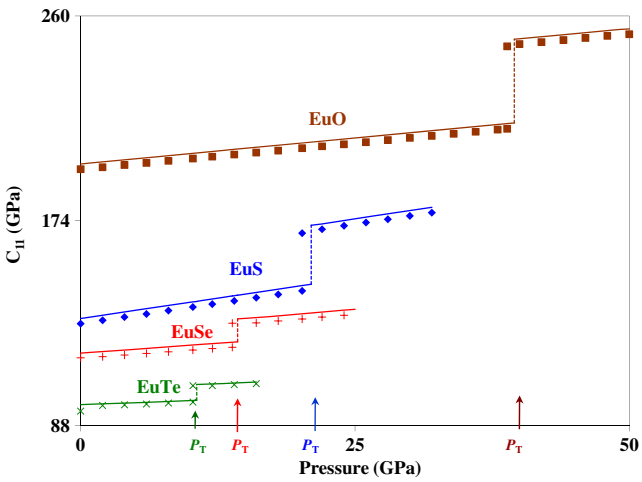

Fig. 9 The variation of C_{11} with pressure (P) for Eu chalcogenides. The *lines* correspond to the MCTP model and the *symbols* to the CTP model

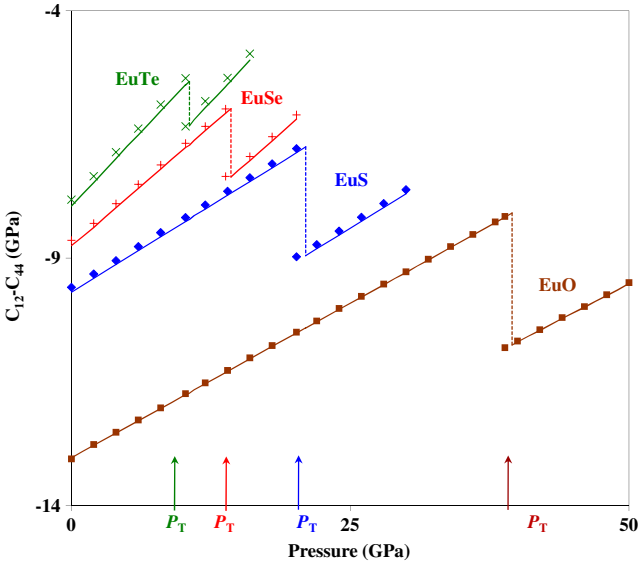

Fig. 10 The variation of C_P (=C_{12} − C_{44}) with pressure (P) for Eu chalcogenides. The *lines* correspond to the MCTP model and the *symbols* to the CTP model

variation of C_{11} with pressure is also depicted in Fig. 9 for EuX, and this shows an abrupt increase at P_T. The decrease in C_{44} (not shown in the figure) indicates that the phase transition is accompanied by shear deformation due to lattice instability. This decrease in C_{44} with applied pressure reflects a significant weakening of the bonding force constant in these materials, which is related to the increase in ionic character with decreasing lattice separation.

The computed values of Cauchy's discrepancy ($C_{12}\neq C_{44}$), also known as the Cauchy pressure (C_P), are plotted in Fig. 10 for the Eu chalcogenides. At zero pressure, our calculated values of C_P from the MCTP (CTP) model show that $C_{12}\neq C_{44}$ in these compounds, which is also observed experimentally in most of the compounds. It was found that these values decrease with increasing chalcogen radius in the B1 phase. The negative value for Cauchy's discrepancy is a consequence of the hybridization of f electrons. This hybridization may be responsible for the decrease in the Eu–X distance. According to Pettifor [33], the value of C_P is typically positive for metallic bonding; if it is negative, the material has directional bonding with angular character. The computed values for C_P are negative for all of the Eu chalcogenides, so this correlation verifies the nonmetallic character of these materials, with directional bonding. It is noticeable that C_P is more negative for EuO and comparatively less negative for EuS→EuSe→EuTe; we can therefore conclude that the covalent character of these materials decreases from EuO to EuTe. The results are qualitatively and quantitatively better than those obtained in earlier works [9, 15–18], and support the effectiveness and validity of the modified expressions. The expressions of Gour et al. [17, 18], Varshney et al. [23], and Srivastava et al. [24] show that $C_{12} - C_{44}$=0, while their results show different values of C_{12} and C_{44}, so their results are not reliable.

Based on our calculated values, Eu compounds appear to be anisotropic, as A is not unity for any of the compounds [34]. It also decreases with pressure, i.e., the anisotropy increases, and these compounds remain anisotropic in the high-pressure B2 phase too. The shear modulus (G) represents the resistance to plastic deformation, while the bulk modulus (B_T) represents the resistance to fracture. The critical value separating brittle and ductile behavior was taken to be $B_T/G\simeq 2.67$ by Frantsevich et al. [34]. Pugh [35] proposed a simple relationship that empirically links their plastic nature with their elastic ratio B_T/G. The critical value that separates a ductile nature from a brittle nature is ~1.75, i.e., if $B_T/G>1.75$ the material is ductile; otherwise it behaves in a brittle manner. In EuX, the calculated value of B_T/G remains below 1.75, so Eu chalcogenides are brittle under ambient conditions and fulfill both criteria. The ductile/brittle nature of the materials can be distinguished on the basis of the Poisson ratio. For a brittle material, the Poisson ratio (σ) must be $\leq$0.33; otherwise the material is ductile. It can be seen that the present value of σ lies below the critical value, so Eu compounds are brittle in the B1 phase. Their brittleness decreases with pressure. These materials are less brittle in the B2 phase. The brittleness of these materials increases with increasing anion size.

Thermoelastic properties

We have evaluated the variation in elastic wave velocity (υ_m) with pressure for the Eu compounds in order to study some of their thermal properties: specific heat, Debye temperature, etc. It was found that υ_m decreases with pressure in both phases. The values of υ_m were used to compute Debye temperatures (θ_D) for the compounds. These values (corresponding to zero pressure) are reported in Table 4. It is clear that the value of θ_D decreases with increasing anion size. A similar decreasing trend has been observed for other members of this family.

Table 4 Calculated values of the Debye temperature (θ_D in K) for Eu chalcogenides at P=0

Property	EuO	EuS	EuSe	EuTe	Reference
θ_D	347	201	149	129	Present work: MCTP
	346	199	148	128	Present work: CTP
	350 [11]	205±16, 203 [13]	153±9	134±10	Expt. [14]

Conclusions

The following conclusions can be drawn from the results of the present calculations:

- These materials are closed-shell ionic systems that crystallize in the $Fm\bar{3}m$ phase group under ambient conditions
- These compounds undergo a first-order transformation from the sixfold-coordinated NaCl (B1) structure to the eightfold-coordinated CsCl (B2) structure
- The calculated mechanical properties—equilibrium volume, transition pressure, EOS / phase diagram and volume collapse at the transition pressure in both phases—are in reasonably good agreement with experimental data, and are more accurate than earlier theoretical results
- The elastic properties also show an abrupt change at P_T, confirming that the phase transition occurs due to structural changes under compression
- The computed thermoelastic properties are in good agreement with the measured data
- EuO is more compressible than EuS, EuSe, and EuTe; in other words, EuTe is the least ductile, and that brittleness increases with increasing anion size.

Acknowledgments The authors are thankful to the department of Science and Technology (DST), New Delhi, for financial support.

References

1. Didchenko R, Gortsema FP (1963) J Phys Chem Solids 24:863–870
2. Singh D, Srivastava V, Rajagopalan M, Husain M, Bandyopadhyay AK (2001) Phys Rev B64:115110–115116
3. Zimmer HG, Takemura K, Syaseen K (1984) Phys Rev B29:2350–2352
4. Jayaraman A (1972) Phys Rev Lett 29:1674–1676
5. Jayaraman A, Singh AK, Chatterjee A, Devi SU (1974) Phys Rev B 9:2513–2520
6. Jayaraman A, Singh AK, Chatterjee A, Devi SU (1972) Phys Rev B 6:2285–2291
7. Rooymans CJM (1965) Solid State Commun 3:421–424
8. Svane A, Santi G, Szotek Z, Temmerman WM, Strange P, Horne M, Vaitheeswaran G, Kanchana V, Petit L, Winter H (2004) Phys Status Solidi B 241:3185–3192
9. Rached D, Ameri M, Rabah M, Khenata R, Bouhemadou A, Benkhettou N, Dine el Hannani M (2007) Phys Status Solidi B 244:1988–1996
10. Wyckoff RWG (1963) Crystal structures. Wiley, New York
11. Shapira Y, Reed TB (1969) J Appl Phys 40:1197–1199
12. Benedict U (1995) J Alloys Compd 223:216–225
13. Benbattouche N, Saunders GA, Bach H (1990) J Phys Chem Solids 51:181–188
14. Subhadra KG, Rao BR, Sirdeshmukh DB (1992) Pramana J Phys 38:681–683
15. Singh D, Rajgopalan M, Bandyopadhyay AK (1999) Solid State Commun 112:39–44
16. Singh D, Rajagopalan M, Husain M, Bandyopadhyay AK (2000) Solid State Commun 115:323–328
17. Gour A, Singh S, Singh RK (2008) Pramana J Phys 71:181–186
18. Gour A, Singh S, Singh RK (2008) J Phys Chem Solids 69:1669–1675
19. Singh RK (1982) Phys Reports 85:259–401
20. Singh RK, Gupta DC (1987) IL Nuovo Cimento D9:1253–1264
21. Motida K (1986) J Phys Soc Jpn 55:1636–1649
22. Hafemeister DW, Flygare WH (1965) J Chem Phys 43:795–800
23. Varshney D, Joshi G, Varshney M, Shriya S (2010) Physica B 405:1663–1676
24. Srivastava AK, Kumaria S, Gupta BRK (2010) Phase Trans 83:28–36
25. Fröhlich H (1949) Theory of dielectrics. Clarendon, Oxford
26. Kittel C (2004) Introduction to solid state physics, 8th edn. Wiley, New York
27. Born M, Huang K (1954) Dynamical theory of crystal lattices. Clarendon, Oxford
28. Slater JC, Kirkwood JG (1931) Phys Rev 37:682–697
29. Singh RK, Gupta DC (1989) Phys Rev B 40:11278–11283
30. Guo YD, Yang ZJ, Gao QH, Liu ZJ, Dai W (2008) J Phys Condens Matter 20:115203–115209
31. Cochran W (1971) Lattice dynamics of ionic and covalent crystals. CRC Crit Rev Solid State Sci 2:1–44
32. Wallace DC (1972) Thermodynamics of crystals. Wiley, New York
33. Pettifor DG (1992) Theoretical predictions of structure and related properties of intermetallics. Mater Sci Tech 8:345–349
34. Frantsevich IN, Voronov FF, Bokuta SA, Frantsevich IN (1983) Elastic constants and elastic moduli of metals and insulators handbook. Naukova Dumka, Kiev
35. Pugh SF (1954) Relations between elastic moduli and plastic properties of polycrystalline pure metals. Phil Mag 45:823–843